Instantaneous RUL Prediction of a Two-Stage Force Feedback Electro-hydraulic Servo Valve (EHSV)

Pratik Punj and Md Adil

1 Introduction

Electro-hydraulic servo valve (EHSV) is one of the most powerful control devices as an outcome of the coupling between electronics and hydraulic power system. They are used to control almost all the hydraulic parameters such as the pressure, pressure difference, angular speeds, etc., with very high precision and speedy responses which makes them highly useful in aviation control system and other sophisticated system which requires high precision and reliability. The most hydraulic fluid used in EHSV can be classified into jet fuel (fuel oil), hydraulic oil and phosphate ester hydraulic oil.

The life span and reliability of EHSV is very vulnerable to the external factors like contamination of hydraulic fluid which leads to the erosion and abrasive wear of the components [1]. Particle erosion wear is ubiquitous while EHSV is operating and is the leading cause of failures [2]. From technical research in this field, it was found that due to the presence of impurities in the circulating hydraulic fluid, the sharp edges of the valve components are washed out, resulting in increased internal leakage flow, input current hysteresis and null leakage, as well as a decrease in input current threshold, pressure gain and gain linearity [3]. Much research has been done qualitatively by analysing the erosive wear (and manufactured geometric error) for the degraded performance of sliding spool [4–6]. Xin Fang established a set of physics-of-failure models for particle erosion wear of EHSV [7], which can help to design an EHSV with high reliability and long life. Ashok K. Singhal created the mathematical basis of the full cavitation model, which showed the effect of cavitation on the service life of hydraulic machines [8]. Yuanbo Chu proposes a

P. Punj (✉)
Department of Mining Machinery Engineering, IIT (ISM) Dhanbad, Dhanbad, India
e-mail: pratik26punj@gmail.com

M. Adil
Department of Mechanical Engineering, Jadavpur University, Kolkata, India

K. M. Singh et al. (eds.), *Fluid Mechanics and Fluid Power, Volume 6*, Lecture Notes in Mechanical Engineering, https://doi.org/10.1007/978-981-99-5755-2_45

dynamic erosion wear characteristics analysis and service life prediction method in which the structural feature and working principle of the nozzle flapper pressure valve are analysed using the brake cavity as the load blind cavity [9]. Wallace MS demonstrated the ability of computational fluid dynamics techniques to study and predict the rate of solid particle erosion in industrially relevant geometries using an Eulerian–Lagrange model of flow in combination with empirically developed mass removal equations to study erosion in valve components in aqueous slurry flows [10]. Paolo Tamburrano et al. 2019 in his paper discussed the operating principle and the analytical models to study EHSV and reported the performance levels using CFD analysis along with the use of smart materials, which aim to improve performance and reduce cost were also analysed in detail [12].

This paper is focused on determining the remaining useful life (RUL) of the EHSV due to erosion wear by studying the nature of the volume flow rate collected through return oil port and then using a machine learning algorithm to determine the RUL of any new similar EHSV at any instant. The volume of return oil is a contribution from three sources: discharge through flapper nozzle assembly, discharge through radial clearance between spool and valve casing and due to the fillet at spool lands and casing ports.

2 Methodology

The mathematical model helps to analyse the effect of erosion wear on the components geometrical structure and how this change effects the overall performance of the valve, so that the degradation of performance can be linked to its life cycle. Figure 1 shows the schematic diagram of a two-stage force feedback EHSV. It consists of two parts namely a pre-amplifier stage that consists of moving-iron torque motor and double nozzle-flapper valve, and a slide valve power amplifier stage.

The armature is supported by spring and is evenly spaced between the upper and lower permanent magnets. The flapper is evenly spaced between the two nozzles. The main spool of the EHSV, which is in the neutral position, has no output.

When Δi is supplied as the electrical input control current to the armature coil, the armature assembly deflects out of position and the flapper moves out of its centre position, blocking flow from one of the nozzles, and due to flow accumulation in the corresponding nozzle, there is a generation of a pressure differential across the spool ends will cause the spool to move from its zero or zero position, opening the EHSV and outputting the appropriate pressure and flow [11]. Reversing the direction of flow correspondingly reverses the direction of flow pressure since valve output magnitude and armature deflection angle are proportional to electric current. In Fig. 1, the i_1, i_2 are the input control currents; P_1, P_2 are the respective pressures at the spool ends; P_s is the supply oil pressure; P_A, P_B are the respective load pressures at ports A and B; P_o is the pressure of the return oil port.

As discussed above, the main contributor in the volume collected at the return oil port are as follows:

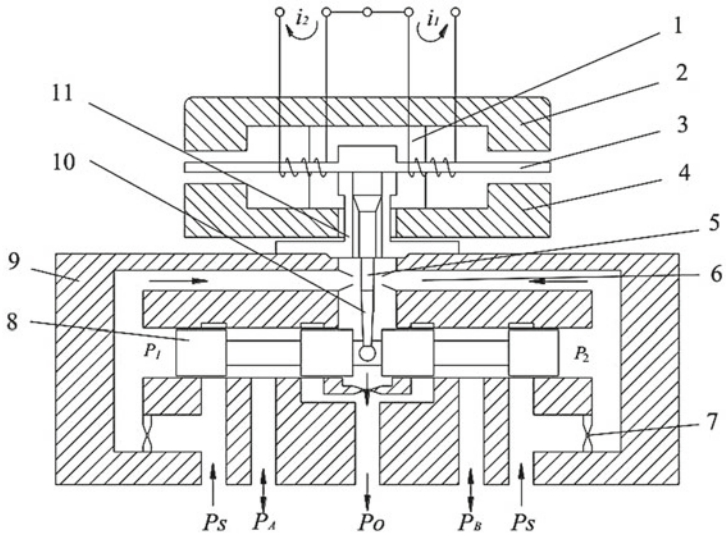

1. control coil; 2. upper permanent magnet; 3. armature; 4. lower permanent magnet; 5. flapper; 6. nozzle; 7. fixed restrictor; 8. main spool; 9. valve sleeve; 10. feedback bar; 11. spring tube

Fig. 1 Schematic diagram of a two-stage electro-hydraulic servo valve [11]

- Leakage flow through nozzle jets
- Leakage flow due to the clearance between spool and sleeve
- Leakage flow due to increase in fillet radius at spool lands and valve ports.

The mathematical models of each of these are discussed below.

2.1 Flow Through Nozzle Jet

From Fig. 2, it is clear that the maximum leakage flow through nozzle exists at the zero position also called as the null position of the flapper. The flow loss and power loss decrease with the change of flapper position.

In Fig. 2, Q_a, Q_b are flow through restrictor a and b, respectively; Q_s be the supply flow into the valve; Q_1, Q_2 be the respective flow through the nozzles 1 and 2, respectively; A is the axial area of the spool land, and U is the velocity with which spool moves. Then

$$Q_s = Q_a + Q_b \tag{1}$$

$$Q_a = Q_1 + AU \tag{2}$$

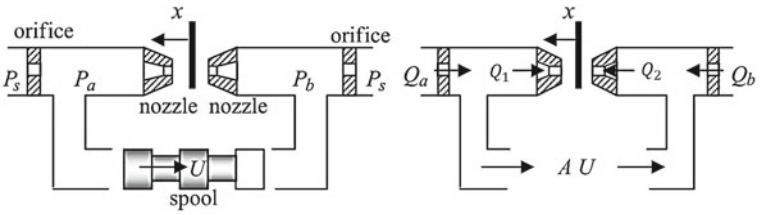

Fig. 2 Flapper nozzle amplifier used to move spool [11]

$$Q_b = Q_2 - AU \tag{3}$$

Since restrictor a and b are orifices, then the flow through them (Q_a, Q_b) are as follows:

$$Q_a = C_{do} \cdot A_o \sqrt{\frac{2(P_s - P_a)}{\rho}}, \quad Q_a = C_{do} \cdot A_o \sqrt{\frac{2(P_s - P_b)}{\rho}} \tag{4}$$

and flow through nozzles 1 and 2 (Q_1, Q_2) are as follows:

$$Q_1 = C_{dn} \cdot A_{n1} \sqrt{\frac{2P_a}{\rho}}, \quad Q_2 = C_{dn} \cdot A_{n2} \sqrt{\frac{2P_b}{\rho}} \tag{5}$$

as shown in Fig. 3,

$$A_o = \frac{\pi}{4} d_o^2 \tag{6}$$

$$A_{n1} = \pi d_n (x_o - x) \tag{7}$$

$$A_{n2} = \pi d_n (x_o + x) \tag{8}$$

x_o = nozzle flapper clearance at null position,
d_o = diameter of restrictor orifice,
d_n = diameter of nozzle.

While in operation the movement of spool is very small and slow so, we can neglect its effect, i.e. taking $AU = 0$, then $Q_a = Q_1 = Q_2 = Q_b$. This leads to

$$\overline{P_a} = \frac{1}{1 + z(1 - \overline{x})^2} \quad \text{and} \quad \overline{P_b} = \frac{1}{1 + z(1 + \overline{x})^2} \tag{9}$$

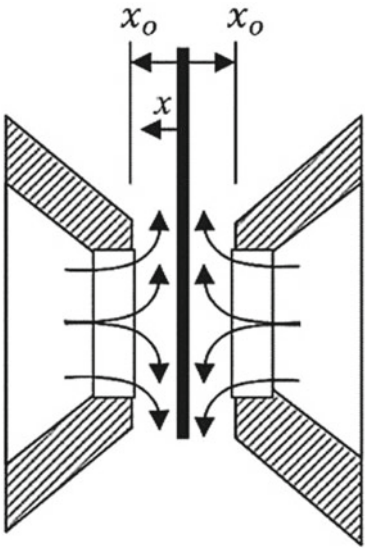

Fig. 3 Flapper nozzle schematic

where $\overline{P_a} = \frac{P_a}{P_s}$; $\overline{P_b} = \frac{P_b}{P_s}$; $\overline{x} = \frac{x}{x_o}$; $z = 16\left(\frac{C_{qn}}{C_{qo}}\right)^2\left(\frac{d_n}{d_o}\right)^2\left(\frac{x_o}{d_o}\right)^2$.

So, the pressure differential is

$$\Delta\overline{P} = \overline{P_a} - \overline{P_b} = \frac{4z\overline{x}}{\left[1 + z(1-\overline{x})^2\right]\left[1 + z(1+\overline{x})^2\right]}$$

and the total flow loss through the two nozzles are as follows:

$$\overline{Q_l} = \frac{(1-\overline{x})}{\sqrt{1 + z(1-\overline{x})^2}} + \frac{(1+\overline{x})}{\sqrt{1 + z(1+\overline{x})^2}} \tag{10}$$

At null position, i.e. $\overline{x} = 0$, $\Delta\overline{P} = 0$, then $\overline{P_a} = \overline{P_b} = \frac{1}{(1+z)}$ and the null pressure gain $= \frac{\mathrm{d}\Delta\overline{P}}{\mathrm{d}\overline{x}} = \frac{4z}{(1+z)^2}$.

The maximum null gain is obtained at $z = 1$ which suggest that at null pressures $P_a = P_b = \frac{P_s}{2}$ and $\overline{Q_l} = \sqrt{2} = 1.414$. The total leakage flow due to the flapper–nozzle assembly is

$$Q_{ln} = \overline{Q_l} \cdot k_n \tag{11}$$

where

$$k_n = C_{dn} \cdot \pi d_n x_o \sqrt{\frac{2P_s}{\rho}}. \tag{12}$$

From the earlier research works, it is reasonable to select the nozzle flow coefficient (C_{dn}) to be 0.62 and the orifice flow coefficient (C_{do}) to be of value 0.79. The orifice diameter generally varies between 0.15 and 0.4 mm, nozzle diameter varies between 0.45 and 0.7 mm, and the flapper clearance varies very little around 0.03 mm.

2.2 Flow Through Radial Clearance of Spool Valves

Due to the sliding of spool, the erosion wear occurs and the radial clearance between spool and sleeve increases with time resulting in the increase of leakage flow through the return port. Considering the valve set are ideal and there only a radial clearance exist as shown in Fig. 4 and when the load flow is zero, the maximum leakage flow can be expressed by a mean flow, which is laminar when the flow is through the sharp-edged orifices.

So, the leakage flow through the radial clearance can be expressed as

$$Q_c = \frac{\pi W c^2}{32\mu} \cdot \Delta P \tag{13}$$

where $W = nw =$ total port area gradient, w is the single port area gradient, μ is the dynamic viscosity of the hydraulic fluid, ΔP is pressure between the spool, c is the radial clearance.

At null position flow through each orifice is $\frac{Q_s}{2}$ and pressure drop is $\frac{P_s}{2}$. Then

$$Q_c = \frac{\pi W c^2}{32\mu} \cdot P_s \tag{14}$$

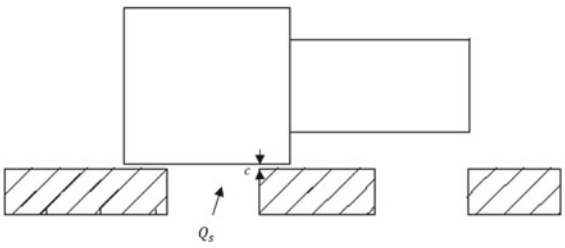

Fig. 4 Spool with radial clearance only

2.3 Leakage Flow Due to Spool Valve Fillet

Due to the manufacturing limitations, even a new spool valve has a rounded corner or fillet at its edges and cannot go below 0.5 μm of fillet radius. Due to the flow recirculation, cavitation and erosion wear due to contaminated fluid, these sharp edges wear out and the fillet radius increases with time. Considering only rounded corners of equal radius and zero radial clearance as shown in Fig. 5, the orifice length (l_f)

$$l_f = \sqrt{(2r)^2 + (2r)^2} - (2r) \tag{15}$$

And the leakage flow through them is as follows:

$$Q_f = \frac{\pi W l_f^2}{32\mu} \cdot P_s \tag{16}$$

The leakage flow through the combination of both clearances as well as valve fillets is the following:

$$Q_{fc} = \frac{\pi W l^2}{32\mu} \cdot P_s \tag{17}$$

where $l = \sqrt{(2r + c)^2 + (2r)^2} - (2r)$ as shown in Fig. 6. So, the total flow rate through the return oil port is given by: $Q_r = Q_{ln} + Q_{fc}$.

3 Using ML Model for Instantaneous RUL Prediction

Using the above relations, a data sheet is created that contains the values that varies with time. Then, this data sheet if fed to a ML algorithm which is then used to calculate the instantaneous RUL. The predictors are return oil flow rate, supply pressure, fluid density and viscosity while the response is the time. This predicted time is used to calculate the RUL by subtracting it from the time of failure at that supply pressure, density and viscosity. The algorithm of the ML model is explained in Fig. 7.

From the data sheet created the predictor and response is selected and is split into training and testing dataset. Training data is fed to KNN Regressor with 1 neighbour and then training and testing RMSE is calculated. If the $\text{RMSE}_{\text{Test}} < \text{RMSE}_{\text{Training}}$, then the model can be used for making prediction on new sample and if $\text{RMSE}_{\text{Test}} > \text{RMSE}_{\text{Training}}$ then the number of neighbours is increased until $\text{RMSE}_{\text{Test}} < \text{RMSE}_{\text{Training}}$. Now, this final ML model is used to calculate the instantaneous RUL with the new sample in the same sequence as that of predictor.

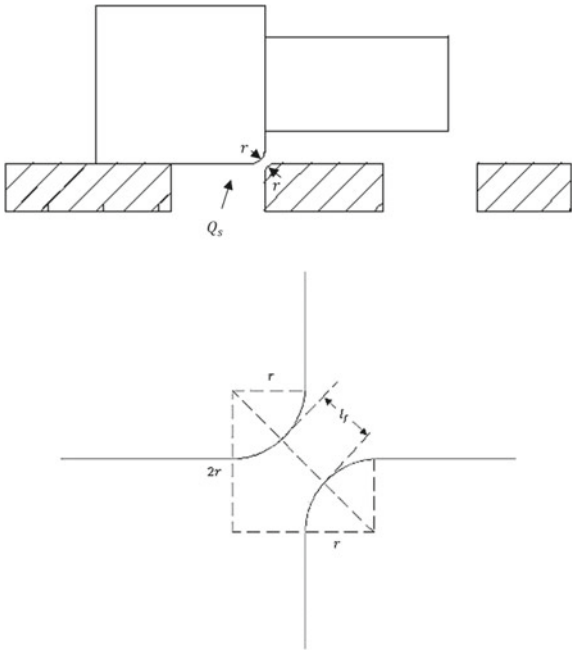

Fig. 7 KNN regression model for prediction RUL

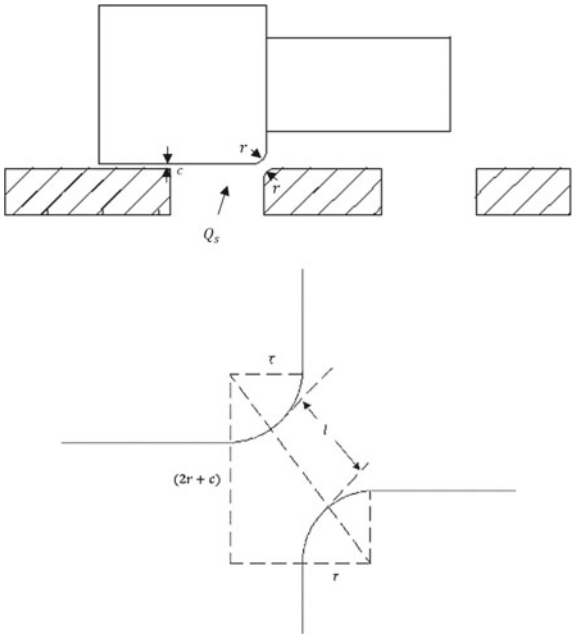

Fig. 6 Spool with both radial clearance and worn orifice

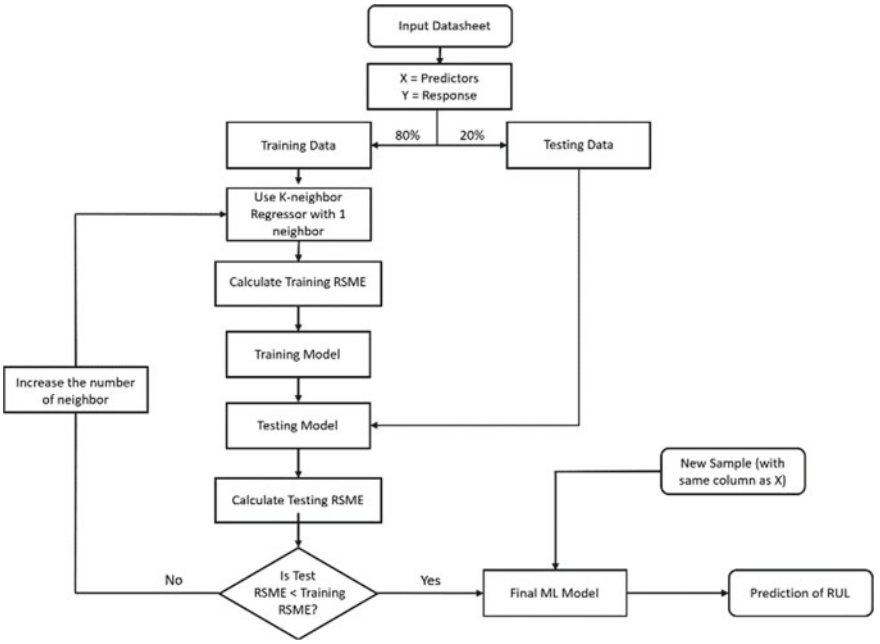

Fig. 5 Spool with worn orifice only

4 Simulation and Results

To proceed with the simulation and finding the variation and dependency of fillet radius, radial clearance as well as the failure time of the valve, the parameters are obtained with reference to the research article [7]. The data are as follows:

Parameter	Marks	Value
Discharge coefficient of nozzle	C_{dn}	0.62
Supply pressure	P_s	100–210 bar
Hydraulic fluid density	ρ	850 kg/m^3
Dynamic viscosity of hydraulic fluid	μ	0.01257 kg/m s
Slot orifice length	w	2.641 mm
Total slots length	W	10.564 mm
Nozzle inner diameter	d_n	0.5 mm
Radial clearance of spool and sleeve	c	2.2 mm
Clearance between nozzle and flapper	x_o	0.03125 mm
Threshold value of internal leakage flow	Q'_r	2.5 lpm

Initial fillet radius is increased by the reverse flow and the presence of cavitation which results in the contamination of hydraulic fluid and there is rapid increase

of the fillet radius due to the fluid contamination. So, a quadratic relation between fillet radius and time is assumed according to the data from research article [7]. The relationship is as follows:

$$r(t) = 1.75 \times 10^{-6} t^2 + 0.001t + 0.604$$

With the increase in fillet radius and fluid contamination, the radial clearance also increases. For this assuming a linear relationship with the increase in fillet radius:

$$c = 0.477r + 1.9136$$

Due to the fluid contamination, the nozzle diameter also increases (although very small). Considering the linear relationship of increase in nozzle diameter with time as:

$$d_n = 3.513 \times 10^{-5} t + 0.5$$

Putting the above three equations, the final return oil flow rate for different supply pressures is as shown in Fig. 7. The plot shows the quadratic relationship with time for the return oil flow collected form return oil port, although the nature is not accurate as that of the actual data collected from the return oil port which shows the linear dependency of return oil flow with time. The comparison is shown in Fig. 8 at 210 bar supply pressure. Although a lot of variation is present in middle portion at the threshold value of 2.5 lpm (as per the design), the MM (Mathematical model) reached the threshold before the actual with RMSE of 0.41.

Using the above data, a database (shown in Fig. 10) is created with time, return oil flow rate, supply pressure, density of fluid, dynamic viscosity of fluid, and with the use of machine learning tool KNN regression, with return oil flow rate, supply

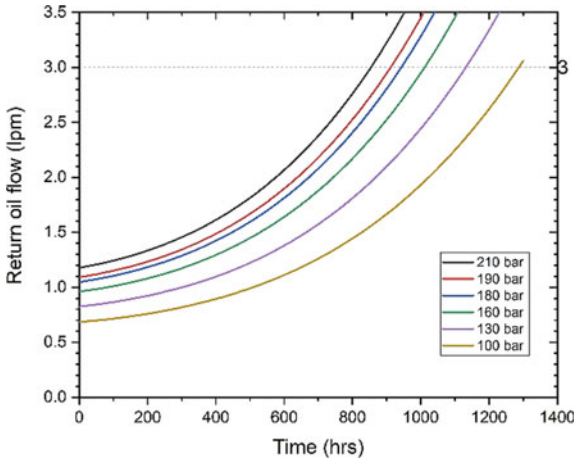

Fig. 8 Comparison of return oil flow at different supply pressures as per mathematical model

pressure, fluid density, dynamic viscosity, as predictors and time as response, the instantaneous RUL can be calculated taking in account the time required to reach the threshold return oil flow volume (3.0 lpm) for the particular supply pressure. The R^2 score of the KNN regression with 2 neighbours is 0.999448297.

5 Conclusions

Using the nonlinear variation of wear with time, a mathematical model is created above to estimate the contribution of different sources in the return oil flow rate collected from the port in EHSV. Although the plot from Fig. 9 shows that the flow rate calculated by MM varies quadratically with time, the actual flow rate is showing a linear relationship but still both showed the same failure time. A database is created using the data from MM at different supply pressures, and a ML model is used to predict the instantaneous RUL by using the required data from the new EHSV (Fig. 10).

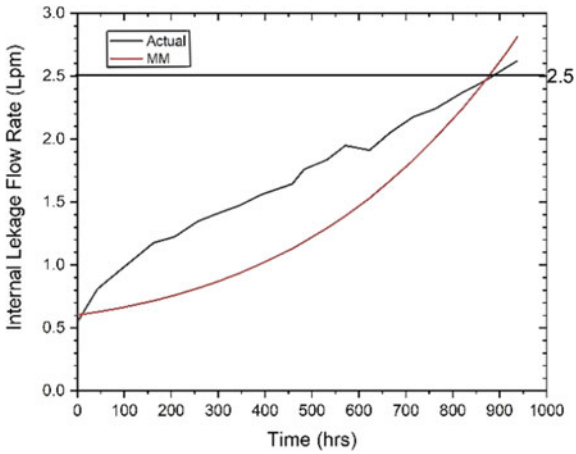

Fig. 9 Comparison between actual and predicted with mathematical model

	Time	radius	clearance	Internal_Leakage	Nozzle_leakage	Total	Pressure	Density	viscosity
0	0.000000	0.604000	2.201708	0.603491	0.573954	1.177446	210	850	0.01257
1	8.686869	0.612819	2.205915	0.607935	0.574305	1.182240	210	850	0.01257
2	17.373737	0.621902	2.210247	0.612541	0.574655	1.187197	210	850	0.01257
3	26.060606	0.631249	2.214706	0.617313	0.575005	1.192318	210	850	0.01257
4	34.747475	0.640860	2.219290	0.622252	0.575356	1.197608	210	850	0.01257

Fig. 10 Datasheet for ML modelling

```
# put sample data in order [Total Leakage Volume, Supply Pressure, Density of Hydraulic Fluid, Dynamic Viscosity of fluid]
x_t = np.array([[1.7,210,850,0.01257]])

for i in range(len(T_f[0,:])):
    if x_t[0,1] == T_f[0,i]:
        break

t_f = T_f[1,i]
y_t = knn.predict(x_t)
RUL = t_f - y_t
print('Current used time is',y_t,'and the avg. failure time for',x_t[0,1],'bar pressure is',t_f,'. RUL is',RUL)
```

```
Current used time is [[447.37373737]] and the avg. failure time for 210.0 bar pressure is 859 . RUL is [[411.62626263]]
```

Fig. 11 Instantaneous prediction of RUL using ML model in python

A robust model can be created by collecting experimental return oil flow data at different supply pressure, density of working fluid, dynamic viscosity of fluid and then creating the database using the ML prediction on those data and then with the help of another ML model predicting the instantaneous RUL (Fig. 11).

Nomenclature

Q_S	Supply flow into valve (lpm)
Q_a, Q_b	Flow through restrictor (lpm)
A	Axial area of spool (mm^2)
A_o	Area of orifice (mm^2)
A_n	Area of nozzle (mm^2)
U	Spool velocity (mm/s)
w	Single port area gradient (mm)
d_o	Diameter of restrictor orifice (m)

References

1. Nystad BH, Gola G, Hulsund JE, Roverso D (2010) Technical condition assessment and remaining useful life estimation of choke valves subject to erosion. In: Annual conference of the PHM Society, vol 2
2. Fitch EC, Ing T (2004) Hydraulic system design for service assurance. BarDyne, Incorporated
3. Zhang K, Yao J, Jiang T (2014) Degradation assessment and life prediction of electro-hydraulic servo valve under erosion wear. Eng Fail Anal 36:284–300
4. Vaughan ND, Pomeroy PE, Tilley DG (1998) The contribution of erosive wear to the performance degradation of sliding spool servovalves. Proc Inst Mech Eng Part J: J Eng Tribol 212(6):437–451
5. Xin Bi H, Yong Yao J, Li Y (2011) Research to the wear and geometric error relations of electro hydraulic servo valve. Procedia Eng 15:891–896
6. Fang X, Yao J, Yin X, Chen X, Zhang C (2013) Physics of-failure models of erosion wear in electrohydraulic servovalve, and erosion wear life prediction method. Mechatronics (Oxf) 23(8):1202–1214
7. Zhang L, Luo J, Yuan RB, He M (2012) The CFD analysis of twin flapper-nozzle valve in pure water hydraulic. Procedia Eng 31:220–227

8. Singhal AK, Athavale MM, Li H, Jiang Y (2002) Mathematical basis and validation of the full cavitation model. J Fluids Eng 124(3):617–624
9. Zhang H, Xiong SB, Liang YW, Xiong X (2008) Analyses of erosion wear characteristic and structure research on hydraulic valve. J China Coal Soc 33(2):214–217
10. Wallace MS, Dempster WM, Scanlon T, Peters J, McCulloch S (2004) Prediction of impact erosion in valve geometries. Wear 256(9–10):927–936
11. Watton J (2014) Fundamentals of fluid power control. Cambridge University Press, Cambridge, England
12. Tamburrano P, Plummer AR, Distaso E, Amirante R (2019) A review of electro-hydraulic servovalve research and development. Int J Fluid Power 20(1)